ISSN 0010-5082, Combustion, Explosion, and Shock Waves, 2020, Vol. 56, No. 6, pp. 705–715. © Pleiades Publishing, Ltd., 2020.
Russian Text © A.P. Ershov, N.P. Satonkina, A.V. Plastinin, A.S. Yunoshev.

Diagnostics of the Chemical Reaction Zone in Detonation of Solid Explosives

A. P. Ershov[a], **N. P. Satonkina**[a,b],
A. V. Plastinin[a], **and A. S. Yunoshev**[a,b]

UDC 544.454.3: 534.222.2: 662.215.2: 662.216.3: 662.237.3

Published in *Fizika Goreniya i Vzryva*, Vol. 56, No. 6, pp. 95–106, November–December, 2020.
Original article submitted October 7, 2019; revision submitted March 17, 2020; accepted for publication June 1, 2020.

Abstract: In studies of the structure of the reaction zone in detonation waves of high explosives, it is common to measure the mechanical characteristics of the flow—the histories of particle velocity, pressure or density. Experience has shown that in such profiles, it is difficult to identify the chemical reaction zone. These distributions, as a rule, are distorted when the flow interacts with measuring systems. In this paper, we consider the prospects of an alternative electrical conductivity method, which is largely free from the above disadvantages and has a number of advantages. The correlation between the region of high electrical conductivity and the reaction zone is validated by comparing the results of conventional methods and conductivity profiles.

Keywords: detonation, condensed explosives, chemical reaction zone, von Neumann spike, electrical conductivity, conduction, carbon nanostructures, conductive networks.

DOI: 10.1134/S0010508220060106

INTRODUCTION

The chemical reaction zone is a region of detonation waves which is the most difficult to investigate. Aggressive environment with high thermodynamic parameters, combined with a short reaction time (about 100 ns or less), greatly limits the range of suitable research methods. According to the Zel'dovich–Neumann–Döring (ZND model), the reaction starts behind the shock front and ends at the Chapman–Jouguet (CJ) point, where the velocity of the material in the frame of reference attached to the front is equal to the local speed of sound [1–3]. At the shock front, the pressure and particle velocity are maximal, and during the reaction, they decrease to the values in the CJ state, so that the distributions of these parameters should contain the von Neumann spike. Since the historically first attempts to clarify the structure of detonation waves [4, 5], this region of increased parameters has been investigated in most experimental studies.

The CJ point (end of the reaction zone) was first sought as an inflection in the corresponding profile. Later it became clear that this assumption is not always valid (this is discussed in more detail in the next section). Therefore, whenever possible, a series of experiments are carried out with different gas-dynamic conditions, e.g., with charges of different lengths. Since the rarefaction wave does not penetrate the CJ sonic point, the region of the profile not subject to changes is taken as the reaction zone.

Measurements of mechanical parameters lead to strong perturbations of the state of material in the reaction zone, which are different for different experimental methods. It is not surprising that the duration of the reaction zone obtained using different techniques and approaches may differ by an order of magnitude [5–11], which stresses the need to develop research methods alternative to those currently used. For the asymptotic, rather slow completion of the reaction, the sonic point can shift depending on the expansion conditions of detonation products [12]. In [8, 9], this effect is considered to be responsible for the marked differences in reaction times measured for charges of different sizes.

---

[a] Lavrent'ev Institute of Hydrodynamics, Siberian Branch, Russian Academy of Sciences, Novosibirsk, 630090 Russia; snp@hydro.nsc.ru.
[b] Novosibirsk State University, Novosibirsk, 630090 Russia.

The lack of a generally accepted method for identifying the von Neumann spike associated with the chemical state of material and hence the lack of reliable information has given impetus to the development of detonation modeling using empirical reaction macrokinetics. The reaction rate is usually given by a rather complex function containing a certain number of adjustable parameters. Initially, there were four to five such parameters [13, 14], and later their number increased significantly (e.g., in [15] there are 15 such parameters). However, most of the currently used models of macrokinetics are not focused on reproducing the structure of the reaction zone. The focus is on the capability of simulating technically important characteristics of material, such as the development of detonation initiated by shock waves, acceleration of metal shells, flows under complex gas-dynamic conditions encountered in practice. Experience has shown that such engineering requirements can be met by very different kinetic models, as evidenced by their large number. Comparison of a number of common kinetics carried out in [16] has shown that within the expected reaction zone, such models do not agree with each other and with experiment.

In the more consistent procedure apparently first used in [17], the selection of kinetics includes the requirement to describe the chemical reaction zone during its interaction with the measuring system. Comparison of calculations and interferometric measurements of the particle velocity of the foil accelerated by a detonation wave made it possible to tune the macrokinetics: only two kinetic parameters were sufficient for reproducing both the shape of the von Neumann spike and detonation initiation. Unfortunately, this approach has not become widespread. Recent studies [10, 11], though providing a significant improvement in methods for measuring flow parameters, have not paid attention to the correct interpretation of data by modeling the entire process, including the reaction zone.

It is known that the detonation of condensed explosives leads to the occurrence of noticeable electrical conductivity [18, 19]. However, for a long time, the use of this effect for the diagnostics of the detonation process was hindered by the insufficient space–time resolution of available measurement methods and by differences in views on the nature of electrical conductivity in detonation waves. We have developed a high-resolution method which has been used to obtain data for a wide range of materials [20–26]. It has been found that for many explosives, conductivity profiles contain narrow peaks that can be reasonably explained by nonequilibrium processes in the reaction zone. Our recent results have allowed us to identify the leading conductivity mechanism that explains available experimental data (see the Discussion section). Thus, the electrical conductivity method opens the prospect of direct investigation of the structure of detonation waves and, in particular, the reaction zone.

In this paper, the influence of chemical reaction kinetics on particle velocity and pressure profiles is illustrated using simulation and conditions for the existence of an inflection in these profiles are given. The results of various measurements of the mechanical parameters of flow are compared with electrical conductivity profiles behind the detonation front for condensed explosives at various initial densities.

INFLUENCE OF KINETICS ON PARTICLE VELOCITY PROFILE SHAPE

As noted above, in early studies of the structure of the detonation front, it was expected that the reaction zone should be clearly distinguished in gas-dynamic profiles; i.e., the end of the reaction should correspond to an inflection in the time dependence of the particle velocity U. This behavior does not follow from ZND theory, although it can be observed under certain assumptions about the shape of the energy release kinetics. Below we show that for the existence of a singularity, a sufficiently fast decrease in the reaction rate near the CJ point is necessary.

In most of the macrokinetics used, the rate of decomposition of explosives is represented as a function of the degree of conversion λ and flow parameters (pressure, temperature or internal energy, etc.) As a rule, in the vicinity of the CJ point, the reaction rate can be represented as

$$\frac{d\lambda}{dt} = \frac{(1-\lambda)^n}{\tau}, \tag{1}$$

where $\lambda = 0$ corresponds to the shock front, $\lambda = 1$ to the end of the reaction, and the characteristic time τ as $\lambda \to 1$ can be considered a constant. In the literature, the exponent n, which determines the presence of a singularity, varies within a fairly wide range—from 0 (sudden termination of the reaction, see, e.g., [27]) to 1, as in [12]. In specific kinetics (e.g., [15, 28]), the right-hand side usually contains several terms of the form (1), which can be included upon reaching certain conditions, with different values of n and different functional dependences for τ. This presumably reflects the sequence of processes taking place in the reaction zone. In the vicinity of the CJ point, the term with the minimum value of n plays a key role, and it is retained in the simplified equation (1).

For illustration, we assume that dependence (1) with a constant value of τ holds during the entire reaction. Then, the explicit solution of (1) for $n < 1$ has the form

$$1 - \lambda = \left(1 - \frac{(1-n)t}{\tau}\right)^{1/(1-n)}.$$

It can be seen that the reaction is completed in the time $t_{\rm J} = \tau/(1-n)$. Near the CJ point, we obtain

$$1 - \lambda \propto (t_{\rm J} - t)^{1/(1-n)}.$$

In experiments, the pressure or particle velocity, rather than the degree of conversion, is measured. Since, at the CJ point, the Rayleigh–Michelson line is tangent to the detonation adiabat, then at a small deviation from this point,

$$U - U_{\rm J} \propto p - p_{\rm J} \propto \sqrt{1-\lambda} \propto (t_{\rm J} - t)^m,$$
$$m = [2(1-n)]^{-1}.$$

For $n = 1/2$, the exponent in the last expression is 1, so that the time dependence of particle velocity is linear. At the end of the reaction, the velocity is ideally constant, but in practice there is a slow decrease in the velocity, which is determined by the expansion of detonation products in the adjacent Taylor wave. This case corresponds to the "classical inflection" expected in early studies. For smaller values of n, the exponent $m < 1$; e.g., $m = 3/4$ for $n = 1/3$. In this case, an inflection also occurs, and it is sharper, from a vertical decline at the end of the reaction to an almost horizontal Taylor dependence. Finally, for $1 > n > 1/2$, the exponent $m > 1$. For example, $n = 2/3$ corresponds to $m = 3/2$, and for this kinetics, there is no inflection and the passage through the CJ point is smooth, but the point itself is not distinguished in the profile. In the case $n = 1$, from Eq. (1) we have

$$1 - \lambda = \exp{(-t/\tau)}$$

and near the Jouguet state,

$$U - U_{\rm J} \propto \exp{[-t/(2\tau)]}.$$

Since, formally, the reaction does not end, an inflection in wave profiles cannot be distinguished. Note that, in this case, the characteristic time of change in dynamic parameters is twice the characteristic reaction time.

To demonstrate the effect of kinetics on the shape of the particle velocity profile, we consider the results of numerical calculations using kinetics (1). The one-dimensional nonstationary problem of detonation initiation by impact of a plate was solved. At the initial time $t = 0$, an RDX charge of initial density 1.7 g/cm^3 occupied a segment of the x axis from 0 to 20 mm. Further, at $x > 20$ mm, there was an inert Plexiglas window. A Lagrangian formulation with the basic equations taken from [27] was used. The material in the reaction zone consists of two components: detonation products with mass fraction λ and unreacted material with fraction $1 - \lambda$. The pressure p in the components is considered the same. For detonation products, we used the Kuropatenko equation of state [29], and for the explosive and Plexiglas, the Mie–Grüneisen equations based on the Hugoniot of the corresponding material, which was given by $D = a + bU$, where D is the shock wave velocity and U is the particle velocity. For the explosive, the parameters were $a = 2.87$ km/s, $b = 1.61$, and a Grüneisen coefficient $\Gamma = 0.85$; for Plexiglas, $a = 2.59$ km/s, $b = 1.52$, and $\Gamma = 0.85$. The explosive was initiated by impact of a plate accelerated to a theoretical velocity at the CJ point $U_{\rm J} = 2.167$ km/s. The plate had a finite mass of 1.18 g/cm^2 (which corresponds to 10 mm of Plexiglas), but in the calculation, it was considered thin. After the impact, the plate slows down, and after a time, reverse motion begins, producing a rarefaction of detonation products.

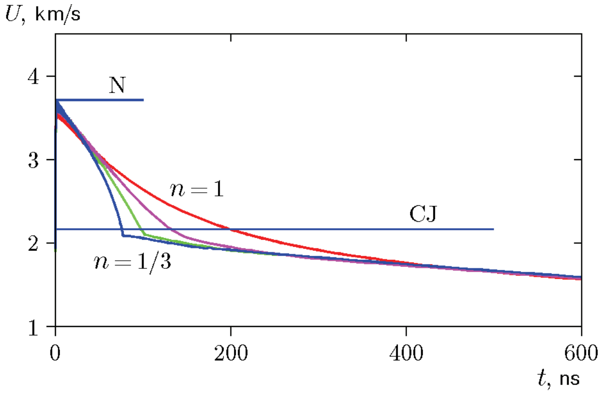

Fig. 1. Particle velocity at the Lagrangian point near the charge end: curves correspond to exponents $n =$ 1, 2/3, 1/2, and 1/3 (from top to bottom); the horizontal lines N and CJ refer to the theoretical Neumann and Chapman–Jouguet levels, respectively.

Figure 1 shows the calculated records of the ideal Lagrangian particle velocity sensor initially placed near the end of the charge (at $x = 17.5$ mm) for a characteristic time $\tau = 50$ ns. The versions $n = 1$, 2/3, 1/2, and 1/3 are shown. It is seen that the numerical calculation confirms the considerations stated above. Clear identification of the chemical reaction zone is possible only for $n \leqslant 1/2$. In this case, inflections in the profile occurs at the times 76 ns ($n = 1/3$) and 101 ns ($n = 1/2$), in good agreement with the expected values of $t_{\rm J} = \tau/(1-n)$, namely, 75 and 100 ns. In Fig. 1, the theoretical velocity levels at the von Neumann spike (N) and at the Chapman–Jouguet (CJ) point are marked. The calculated values at these points are about 3% lower due to numerical errors and incomplete acceleration of

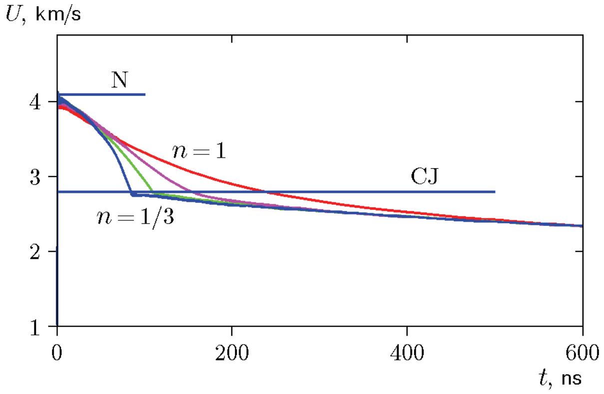

Fig. 2. Calculated velocity profiles at the explosive–Plexiglas interface: the notation the same as in Fig. 1.

the wave (at the moment of measurements, the detonation velocity is approximately 2% lower than the theoretical value of 8.39 km/s). The exponent $n = 1/3$ appears in kinetics [28, 30], and a close value of 2/9 was used in [14]. In [17], $n = 0.545$ (almost 1/2) corresponds to an RDX density of 1.67 g/cm^3.

In contrast, for $n > 1/2$, an inflection in the time dependence is not observed and estimating the reaction time becomes problematic. For $n = 2/3$, one can still use the passage through the CJ level (130 ns), but this estimate differs markedly from the theoretical value of 150 ns. Estimation of the reaction time based on the point where the curve reaches the common asymptote gives a markedly overestimated time of about 250 ns. The exponent $n = 2/3$ appears in the Lobanov model [13] and in a number of other papers, e.g., [15, 31], and was introduced to describe the afterburning of disconnected fragments of the material at the end of the reaction. In [17], a close exponent of 0.7 was selected for an RDX density of 1.6 g/cm^3.

For $n = 1$, the reaction time becomes even more poorly determined. Formally, in this case $t_{\rm J} = \infty$, estimation based on the intersection with the Jouguet level gives about 200 ns, and the linear dependence is visually reached in 400 ns. An attempt to estimate the characteristic time τ by representing the velocity profile as the sum of a linear function and an exponentially decreasing function gives 136 ns, i.e., not far from $2\tau = 100$ ns. Difficulties in determining kinetics at a slowly decreasing reaction rate and the strong influence of the experimental conditions on such measurements are noted in [12]. Kinetics with $n = 1$ were used in [32–34].

In practice, the velocity sensor can be placed not inside the charge, but at the interface with an inert material. For optical velocity measurements having the highest resolution, such setup using a transparent window is the most common. Since the dynamic properties of the explosive and window are different, the velocity of the interface differs from the velocity inside the explosive, which can affect reaction time measurements.

Velocity profiles at the explosive–Plexiglas interface (initial coordinate $x = 20$ mm) for the same exponents are shown in Fig. 2. Here the Neumann and Chapman–Jouguet levels are calculated considering the interaction of corresponding shocks with the window material. The curves are qualitatively similar to the curves in Fig. 1, but all times are somewhat longer than for sensor located inside the explosive. For example, inflections in the profiles occur at $t = 85$ ns ($n = 1/3$) and 115 ns ($n = 1/2$). For $n = 2/3$, the CJ level is intersected in 151 ns (accidental “correction” due to the interaction between the materials), and the linear asymptote is reached in 250 ns. For $n = 1$, the level is intersected in 235 ns, the asymptote is reached in 500 ns, and the characteristic time 2τ estimated based on the exponential and linear approximations gives 195 ns instead of the expected 100 ns.

Thus, if the reaction ends smoothly, measurements can lead to unexpectedly large errors. Note that experiments [7, 8, 10, 11, 35] and a number of others demonstrate rather smooth completion of the reaction. In this case, a noticeable distortion of the characteristic time of the process will be quite typical. In the case of rapid completion of the reaction ($n \leqslant 1/2$), Lagrangian velocity sensors give acceptable results, despite the interaction with the window material. However, it should be noted that our calculation did not include the influence of the wave reflected from the window on the reaction rate in the material. In practice, this influence is undoubtedly present, which complicates the interaction of the detonation zone with the window and introduces additional uncertainty into interpretation of the measurements. The impact of measurements of mechanical parameters on the process under study seems inevitable, so that the results of such measurements should be considered as rather rough estimates.

COMPARISON OF ELECTRICAL CONDUCTIVITY AND PARTICLE VELOCITY PROFILES

The previously developed high-resolution method for measuring electrical conductivity during detonation of condensed explosives is described in detail elsewhere [20]. Here we just note some key points. A charge with a diameter $d_\sigma = 8$ mm is in a thick copper shell with an outer diameter of 40 mm. The time resolution was about 10 ns.

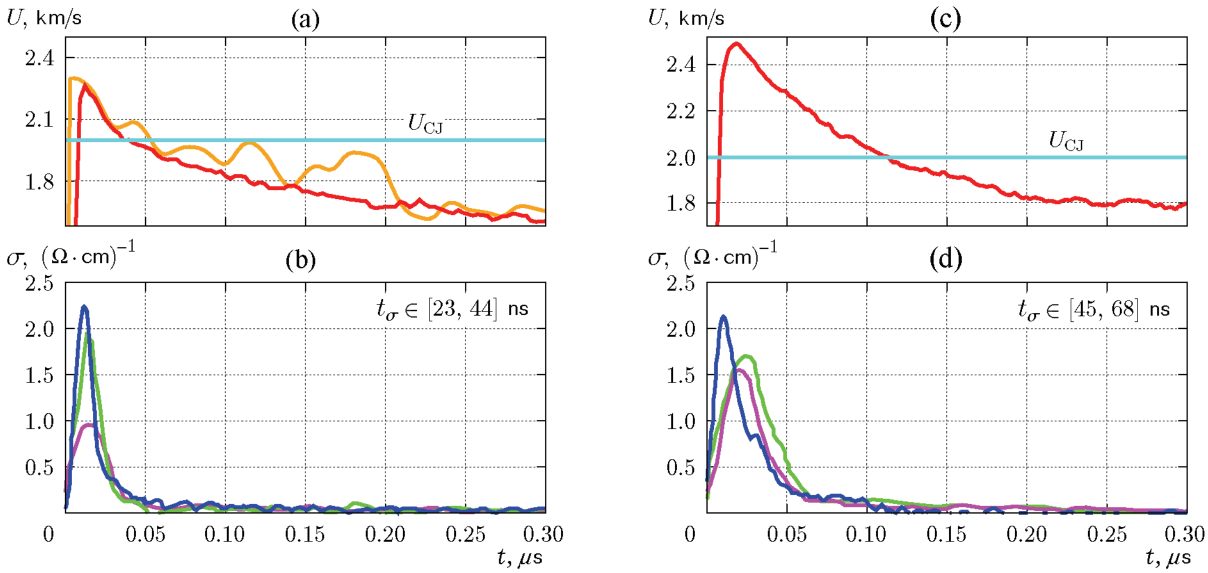

Fig. 3. Data for RDX with a density $\rho = 1.2$ g/cm^3: particle velocity (a and c) and electrical conductivity distribution (b and d) for $d = 11$ (a and b) and 160 μm (c and d).

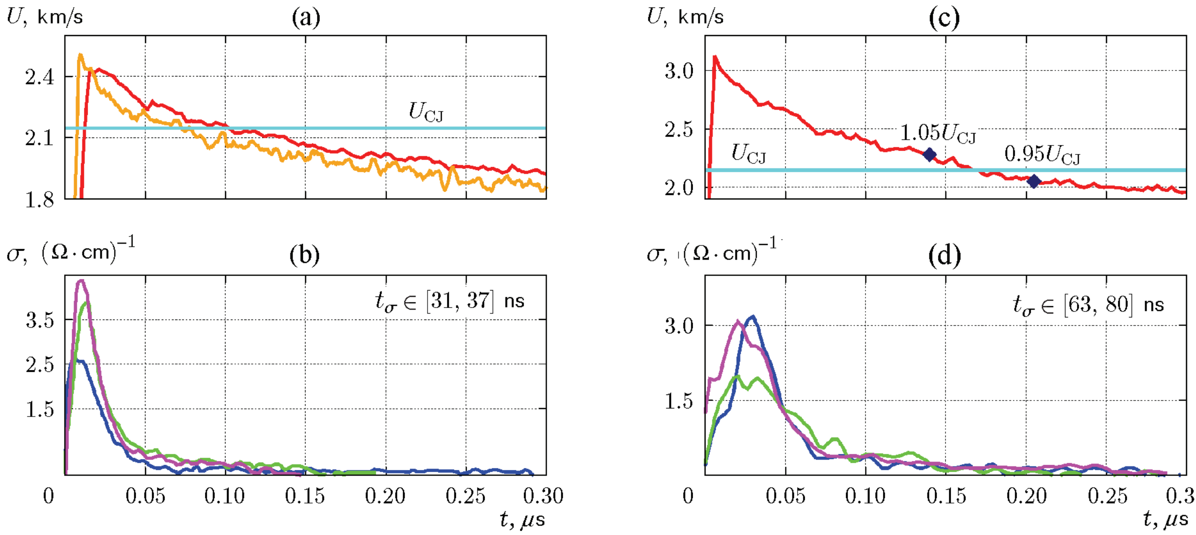

Fig. 4. Data for HMX with a density $\rho = 1.3$ g/cm^3: particle velocity (a and c) and electrical conductivity distribution (b and d) for $d = 21$ (a and b) and 430 μm (c and d).

For detonation of condensed explosives with a moderate carbon content, the typical conductivity profile contains a narrow zone of high values. The sharp peak is followed by a region of low and slowly decreasing conductivity. The electrical conductivity peak, corresponds, in our opinion, to the chemical reaction zone, and the slow decline to the expansion in the Taylor wave. The transitional region has the form of a somewhat smoothed inflection, in which it is natural to localize the CJ point.

A similar pattern of the distribution $\sigma(t)$ is observed for detonation of RDX, HMX, PETN, benzotrifuroxan, and a triaminotrinitrobenzene (TATB) based explosive [20–23, 25] for all densities studied.

Bulk Density Explosive

For low-density explosives, we have our own measurements of particle velocity profiles. As in electrical conductivity measurements, the particle velocity obtained for detonation of charges with a diameter of 8 mm

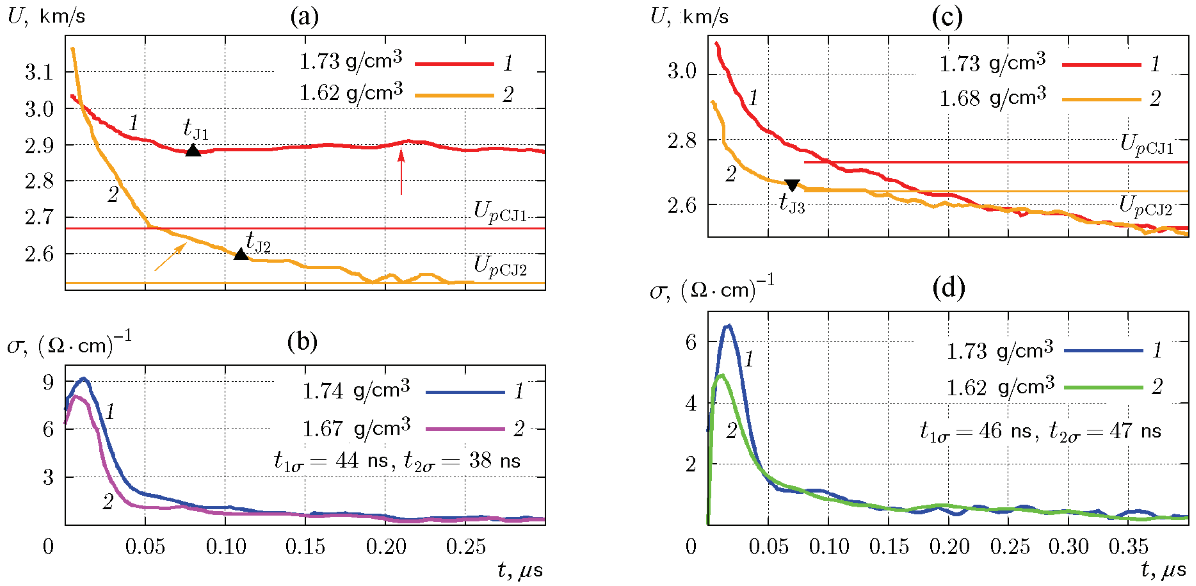

Fig. 5. Data for PETN (a and b) and RDX (c and d): (a, c) $U(t)$ from [17, 18] ($t_{\mathrm{J}1} = 80 \pm 20$ ns, $t_{\mathrm{J}2} = 110 \pm 20$ ns, and $t_{\mathrm{J}3} = 70 \pm 10$ ns); (b, d) $\sigma(t)$ and t_σ.

in a thick copper shell. An aluminum foil 7 μm thick glued to a Plexiglas window at the end of the charge was used as the velocity sensor. Foil velocity was recorded by a VISAR optical system. The procedure is described in more detail elsewhere [36].

Particle velocity $U(t)$ and electrical conductivity $\sigma(t)$ profiles for RDX and HMX are compared in Figs. 3 and 4. The horizontal lines denoted as U_{CJ} indicate the expected velocity of the interface after the interaction with the reacted explosive in the CJ state. We used the CJ parameters calculated in [37], which agree well with experiment [5, 38]. The Hugoniot of Plexiglas was adopted in the form $U_s = 2.59 + 1.52U_p$, where U_s is the shock wave velocity and U_p [km/s] is the particle velocity. For each explosive, three profiles of $\sigma(t)$ are given and the time interval t_σ is specified for the region of high electrical conductivity.

In coarse-grained explosives, electrical conductivity profiles exhibit oscillations due to some inhomogeneity of the charges. However, conductivity peaks are quite distinct. In contrast, the particle velocity signal does not have singularities in the vicinity of the CJ level and in other regions. Curves of $U(t)$ decline smoothly and slowly, so that the moments of intersection with the CJ levels are poorly identified. For example, in coarse HMX, small errors (± 5%) in the CJ level lead to significant deviations in the estimate of the reaction time t_{J}: from 140 to 210 ns, as seen in Fig. 4c. However, both methods demonstrate the same effect of the degree of dispersion: in finely dispersed explosives, both times t_σ and t_{J} are about half as much as in coarsely dispersed explosives. Therefore, both signals track the chemical reaction, but there are differences between them: the time t_{J} systematically exceeds t_σ. This issue is discussed below.

Thus, the conductivity profiles show a high contrast between the peak and the subsequent background level, which allows one to obtain well-determined times t_σ with satisfactory reproducibility. In contrast, the particle velocity profiles do not have evident singularities that allow one to identify the reaction zone, and the contrast of this signal is rather weak.

Dense Explosives

Materials of high density are of great practical importance. We compare our electrical conductivity data with particle velocity profiles at the explosive–chloroform interface obtained in [7] by a photometric method. This paper presents measurement results for many explosives, including those discussed above. The curves of $U(t)$ for PETN and RDX with a charge diameter of 40 mm are shown in Figs. 5a and 5c, and profiles of $\sigma(t)$ at practically the same initial densities in Figs. 5b and 5d. In [7], the time t_{J} was determined as the moment of transition from the exponential to linear decay of the curve. Profiles of $U(t)$, as in the case of low densities, do not have clear signs of the CJ state and their contrast is poor, whereas the conductivity peaks are clearly distinguished. The durations of the regions of high electrical conductivity t_σ are also less than t_{J}.

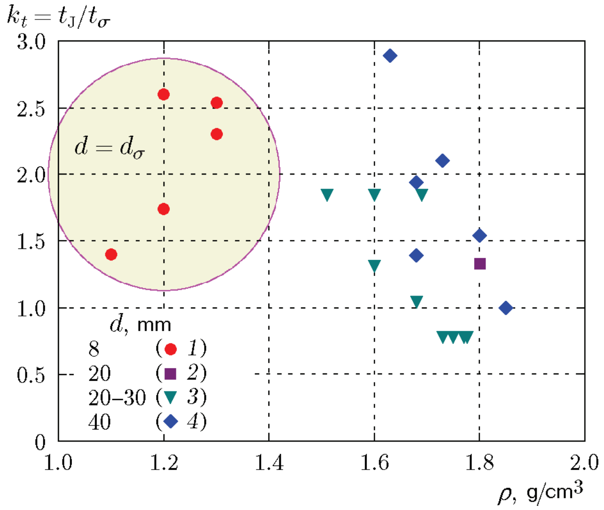

Fig. 6. Ratio of the duration of the reaction zone for detonation of a charge of diameter d to the duration of the high electrical conductivity zone $k_t = t_J/t_\sigma$: points *1* refer to data of [36], points *2* to data of [40, 41], points *3* to date of [39], and points *4* to data of [7].

Smooth dependences similar to the data [7] were obtained, e.g., in [39] using the VISAR method. Characteristic moments in the velocity profiles, if observed, were rather uncertain.

Consequently, in dense explosives, the results based on measurements of mechanical parameters also have a weak contrast, which allows considerable arbitrariness in the localization of the CJ state. Conductivity peaks are distinguished much more reliably.

Figure 6 compares the currently available "dynamic" reaction times t_J given for pure explosives in [7, 36, 39–41], with the times t_σ obtained in our experiments.

Against the background of a significant scatter on the vertical, the "mechanical" times are on average one and a half to two times longer than the corresponding t_σ.

DISCUSSION

One of the reasons why the mechanical time t_J is longer than t_σ may be the difference between the Lagrangian time measured by interferometric methods [8, 9, 23, 36] and photometry [7] and the Eulerian time t_σ. Therefore, to compare the results, it is more correct to use not the time but the width of the electrical conductivity peaks $X_\sigma = Dt_\sigma$ and the linear sizes of the reaction zones given in the literature, $X_J = (D - \langle U \rangle)t_J$. Here $\langle U \rangle$ is the average particle velocity within the von Neumann spike. Figure 7a shows a graph of the ratio $k = X_J/X_\sigma$ for different densities of PETN, RDX, and HMX. Here, as for Fig. 6, we used data from [7, 36, 39–41], where, as in our experiments, pure explosives were studied. Although there is a noticeable scatter of points in Fig. 7a, they are grouped around the level $k = 1$; the average for all data is 1.06.

The scatter of points in Fig. 7a is generated mainly by arbitrariness in the determination of the times t_J and sizes X_J. Slow and smooth decline in the velocity of the interface and the absence of a clear singularity at the CJ point can lead to large errors. The above simulation shows that under such conditions, estimates of t_J deviate markedly from the true values even when using ideal sensors. An additional factor may be the distortion of the wave due to the reflection from the explosive–window interface. Note that for our electrical conductivity method, such distortions are minimal since the wave moves along the surface of the electrodes, and only a slight expansion of the massive metal shell can affect the gas dynamics of the flow.

Thus, the discrepancy between the sizes X_J and X_σ is due to the uncertainty in mechanical measurements t_J. It can be assumed that the quantities t_σ and X_σ reflect the chemical reaction kinetics more reliably.

Comparison with plastic-bonded compositions based on the same explosives is of interest. The results of such a comparison are shown in Fig. 7b. Since, in our experiments, such compositions were not studied, as X_σ we used the data for pure explosives of the same density. There is some decline in the ratio $k' = X_J/X_\sigma$; in some cases, it is less than 0.1, and on average, $k' \simeq 0.3$. Thus, in plastic-bonded compositions, the reaction is accelerated in comparison with pure explosives. To explain this shift, we note that the initial density is not the only or the most important parameter that determines the reaction rate in a detonation wave. Since the reaction starts at hot spots, its course is determined by the structure of the charge and may depend on the initial grain size, the presence of additives, and the procedure used to prepare the charge. A good illustration is the study [42], in which PETN containing nanosized pores detonated in fairly thin layers (50 μm) and PETN pressed from the initial powder of size 100 μm had a critical thickness of 220 μm. Plastic-bonded explosives, as well as dense samples used, e.g., in [31], are materials different from those used in our conductivity measurements. It would be interesting to study the distribution of electrical conductivity in plastic-bonded explosives.

Preliminary comparison of the times t_J and t_σ was carried out in our study [43]. Due to the difference between Lagrangian and Eulerian times and due to the inclusion of plastic-bonded, explosives, the ratio $t_J/t_\sigma \approx 2$ was obtained. In the present work, a more correct

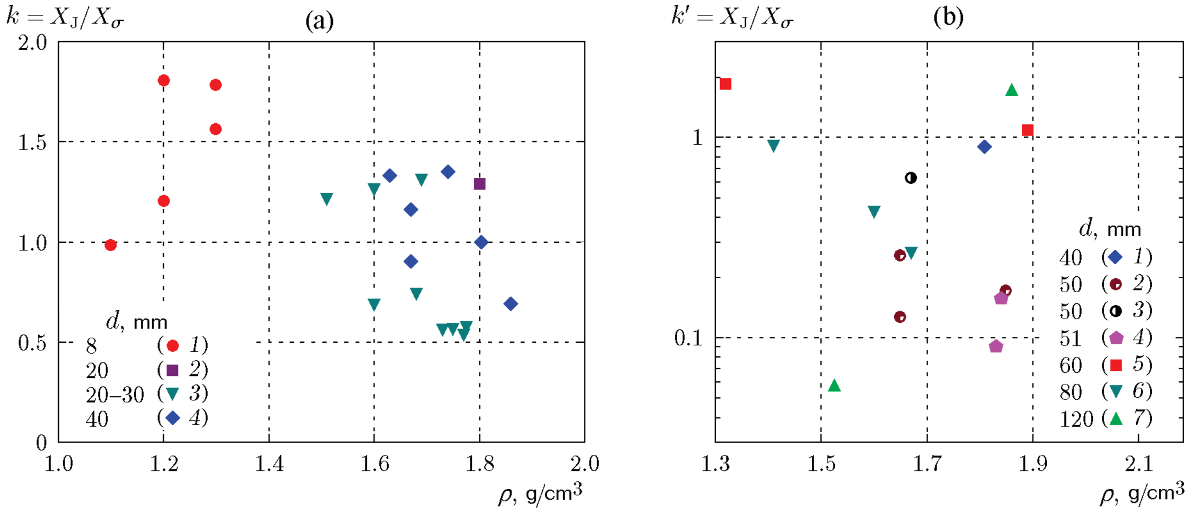

Fig. 7. Ratio of the size of the reaction zone to the width of the conductivity peak $k = X_J/X_\sigma$: (a) notation the same as in Fig. 6; (b) data of [7] (*1* and *5*), [11] (*2*), [10] (*3*), [35] (*4*), [17] (*6*), and [9] (*7*).

comparison was carried out; as a result, the ratio $k = X_J/X_\sigma$ turned out to be close to 1 on average.

A disadvantage of the electrical conductivity method is the lack of a generally accepted concepts of the nature of conduction in the reaction zone. High density and moderately high temperature lead to strong interactions among all particles, which makes a theoretical description of the reacting medium inaccessible.

In recent years, significant progress has been made in this area. In early studies of the electrical properties of detonating explosives, high conductivity values were associated with free carbon. In [19], it was assumed that high electrical conductivity in detonation waves can be explained by the formation of conductive carbon clusters. In [44], conductivity was calculated using the percolation model and the results were compared with the data for TNT. Based on the calculation, it was concluded that extended conductive structures exist already in the chemical reaction zone.

Later, carbon fibers capable of forming conductive networks have been found in detonation products of explosives rich in carbon [45–48]. In principle, even spherical particles can form a conductive network if they are aggregated into a fractal cluster [49].

Our experiments with widely used explosives (RDX, HMX, PETN, benzotrifuroxan, TATB, emulsion explosives) have confirmed the decisive role of carbon [50, 51]. A consistent carbon-based concept was discussed in [52]. Free carbon released after the reaction is responsible for the conductivity in the Taylor wave, with which many authors agree. An important and not obvious aspect is that the conductivity peak can also be explained by the release of free carbon in the reaction zone in an amount exceeding the equilibrium value. This is confirmed by a correlation between the electrical conductivity value and the calculated content of free carbon both at the CJ point and near the von Neumann spike [50, 51]. The idea of rapid decomposition and excess carbon was proposed in [53, 54] by analogy with the shock decomposition of organic explosives and is supported by data on the isotopic composition of detonation products. In the reactions zone, super-equilibrium carbon forms clusters and aggregates, providing maximum electrical conductivity. Later, part of the free carbon is oxidized, resulting in a decrease in the electrical conductivity. This model explains all currently available conductivity data.

CONCLUSIONS

To validate a highly sensitive method for identifying the chemical reaction zone by measuring electrical conductivity, electrical conductivity profiles were compared with the results of conventional research methods—particle velocity profiles. Comparison of various high explosives in a wide range of densities showed that the literature data on the reaction zone sizes are on average close to the width of the corresponding electrical conductivity peaks. The available scatter is mainly due to difficulties in localizing the Chapman–Jouguet state in velocity records. Conditions on the reaction kinetics under which an inflection-type singularity occurs in velocity and pressure profiles were discussed. The absence of such singularities in a number of experimental studies suggests that these conditions are met relatively rarely. At the same time, the contrast of conductivity peaks is much higher. In fact, it is electrical conductivity distributions that have the inflection which was expected in early studies of the structure of reaction zones.

The electrical conductivity method allow, at a modest experimental cost, the identification of changes in the chemical state of material near the von Neumann spike with an acceptable time resolution and with a weak influence on the process under study.

This work was supported by the Russian Foundation for Basic Research (Projects No. 18-03-00227 and No. 18-03-00441).

REFERENCES

1. Ya. B. Zel'dovich, "On the Theory of Detonation Propagation in Gaseous Systems," Zh. Eksp. Teor. Fiz. **10** (5), 542–568 (1940).
2. J. von Neumann, "Theory of Detonation Waves," in *John von Neumann, Collected Works*, Ed. by A. J. Taub (Pergamon Press, New York, 1963), pp. 203–218. (Shock Wave Science and Technology Reference Library, Vol. 6.)
3. W. Döring, "Über den Detonationsvorgang in Gasen [About the Detonation Process in Gases]," Ann. der Physik **43** (6/7), 421–436 (1943).
4. R. E. Duff and E. Houston, "Measurement of Chapman–Jouguet Pressure and Reaction Zone Length in a Detonating High Explosive," J. Chem. Phys. **23** (7), 1268 (1955).
5. A. N. Dremin, S. D. Savrov, V. S. Trofimov, and K. K. Shvedov, *Detonation Waves in Condensed Media* (Nauka, Moscow, 1970) [in Russian].
6. L. V. Altshuler, G. S. Doronin, and V. S. Zhuchenko, "Detonation Regimes and Jouguet Parameters of Condensed Explosives," Fiz. Goreniya Vzryva **25** (2), 84–103 (1989) [Combust., Expl., Shock Waves **25** (2), 209–224 (1989)].
7. B. G. Loboiko and S. N. Lyubyatinskii, "Reaction Zones of Detonating Solid Explosives," Fiz. Goreniya Vzryva **36** (6), 45–64 (2000) [Combust., Expl., Shock Waves **36** (6), 716–733 (2000)].
8. A. V. Fedorov, A. V. Men'shikh, and N. B. Yagodin, "Structure of the Detonation Front in Heterogeneous High Explosives," Khim. Fiz. **18** (11), 64–68 (1999)].
9. A. V. Fedorov, A. L. Mikhailov, L. K. Antonyuk, D. V. Nazarov, and S. A. Finyushin, "Determination of Chemical Reaction Zone Parameters, Neumann Peak Parameters, and the State in the Chapman–Jouguet Plane in Homogeneous and Heterogeneous High Explosives," Fiz. Goreniya Vzryva **48** (3), 62–68 (2012) [Combust., Expl., Shock Waves **48** (3), 302–308 (2012)].
10. J. Pachman, M. Künzel, O. Němec, and J. Majzlík, "A Comparison of Methods for Detonation Pressure Measurement," Shock Waves **28** (2), 217–225 (2018).
11. H. Pei, W. Huang, X. Zhang, and X. Zheng, "Measuring Detonation Wave Profiles in Plastic-Bonded Explosives Using PDV," AIP Adv. **9**, 015306 (2019).
12. S. M. Bakhrakh, A. A. Evstigneev, V. N. Zubarev, and A. A. Shanin, "Influence of the Finite Rate of High-Explosive Decomposition on the Determination of Detonation Parameters," Fiz. Goreniya Vzryva **17** (6), 117–121 (1981) [Combust., Expl., Shock Waves **17** (6), 685–688 (1981)].
13. V. F. Lobanov, "Modeling of Detonation Waves in Heterogeneous Condensed Explosives," Fiz. Goreniya Vzryva **16** (6), 113–116 (1980).
14. E. L. Lee and C. M. Tarver, "Phenomenological Model of Shock Initiation in Heterogeneous Explosives," Phys. Fluids **23**, 2362–2371 (1980).
15. C. M. Tarver, J. W. Kury, and R. D. Breithaupt, "Detonation Waves in Triaminotrinitrobenzene," J. Appl. Phys. **82** (8), 3771–3782 (1997).
16. Yu. A. Aminov, N. S. Es'kov, Yu. R. Nikitenko, and G. N. Rykovanov, "Calculation of the Reaction-Zone Structure for Heterogeneous Explosives," Fiz. Goreniya Vzryva **34** (2), 125–128 (1998) [Combust., Expl., Shock Waves **34** (2), 230–233 (1998)].
17. A. V. Utkin, G. I. Kanel', and V. E. Fortov, "Empirical Macrokinetics of the Decomposition of a Desnsitized Hexogen in Shock and Detonation Waves," Fiz. Goreniya Vzryva **25** (5), 115–122 (1989) [Combust., Expl., Shock Waves **25** (5), 625–632 (1989)].
18. A. A. Brish, M. S. Tarasov, and V. A. Tsukerman, "Electrical Conductivity of Explosion Products of Condensed Explosives," Zh. Eksp. Teor. Fiz. **37** (6)(12), 1543–1549 (1959).
19. B. Hayes, "On the Electrical Conductivity in Detonation Products," in *Proc. of 4th Symp. (Int.) on Detonation, White Oak, MD, 1965, ACR-126* (Office of Naval Research, Washington, 1967), pp. 595–601.
20. A. P. Ershov, N. P. Satonkina, and G. M. Ivanov, "Electroconductivity Profiles in Dense High Explosives," Khim. Fiz. **26** (12), 21–33 (2007) [Russ. J. Phys. Chem. 1, 588–599 (2007); https://doi.org/10.1134/S1990793107060139].
21. A. P. Ershov and N. P. Satonkina, "Investigation of the Reaction Zone in Heterogeneous Explosive Substances Using an Electrical Conductivity Method," Fiz. Goreniya Vzryva **45** (2), 109–115 (2009) [Combust., Expl., Shock Waves **45** (2), 205–210 (2009)].
22. N. P. Satonkina and A. A. Safonov, "Electrical Properties of Trotyl Detonation Products," J. Eng. Thermophys. **18** (2), 177–181 (2009).

23. A. P. Ershov and N. P. Satonkina, "Electrical Conductivity Distributions in Detonating Low-Density Explosives—Grain Size Effect," Combust. Flame **157** (5), 1022–1026 (2010).
24. A. P. Ershov and N. P. Satonkina, "Electrical Conductivity Profiles in Detonating Low-Density Explosives of Various Grain Sizes," in *Proc. of 14th Int. Detonation Symp., Coeur d'Alene, ID, 2010*, ONR 351-10-185 (Office of Naval Research, Arlington, 2010), pp. 302–305.
25. N. P. Satonkina and I. A. Rubtsov, "Distribution of Electrical Conductivity Distribution during Detonation of a TATB-Based Explosive," Zh. Tekh. Fiz. **86** (1), 144–147 (2016) [Tech. Phys. **61**, 142–145 (2016); https://doi.org/10.1134/S1063784216010175].
26. N. P. Satonkina, A. P. Ershov, A. O. Kashkarov, A. L. Mikhaylov, E. R. Pruuel, I. A. Rubtsov, I. A. Spirin, V. B. Titova, "Electrical Conductivity Distribution in Detonating Benzotrifuroxane," Sci. Rep. **8**, 9635 (2018).
27. M. V. Batalova, S. M. Bakhrakh, and V. N. Zubarev, "Excitation of a Detonation in Heterogeneous Explosives by Shock Waves," Fiz. Goreniya Vzryva **16** (2), 105–109 (1980) [Combust., Expl., Shock Waves **16** (2), 227–231 (1980)].
28. V. G. Morozov, I. I. Karpenko, S. E. Kuratov, S. S. Sokolov, B. N. Shamraev, and L. V. Dmitrieva, "Theoretical Justification of a Phenomenological Model of the Shock-Wave Sensitivity of a TATB Based Heterogeneous Explosive Taking into Account Single and Double Shock-Wave Loading along with Intermediate Unloading," Khim. Fiz. **14** (2/3), 32–39 (1995).
29. V. F. Kuropatenko, "Equation of State of Detonation Products of Compact Explosives," Fiz. Goreniya Vzryva **25** (6), 112–117 (1989) [Combust., Expl., Shock Waves **25** (6), 762–767 (1989)].
30. C. M. Tarver, J. O. Hallquist, and L. M. Erickson, "Modeling Short Pulse Duration Shock Initiation of Solid Explosives," in *Proc. of 8th Symp. (Int.) on Detonation* (Albuquerque, NM, 1985), pp. 951–961.
31. C. M. Tarver, R. D. Breithaupt, and J. W. Kury, "Detonation Waves in Pentaerythritol Tetranitrate," J. Appl. Phys. **81** (11), 7193–7202 (1997).
32. J. N. Johnson, P. K. Tang, and C. A. Forest, "Shock-Wave Initiation of Heterogeneous Reactive Solids," J. Appl. Phys. **57** (9), 4323–4334 (1985).
33. W. L. Seitz, J. Stacy, and H. L. Wackerle, "Detonation Reaction Zone Studies on TATB Explosives," in *Proc. of 8th Symp. (Int.) on Detonation* (Albuquerque, NM, 1985), pp. 123–132.
34. J. W. Kury, R. D. Breithaupt, and C. M. Tarver, "Detonation Waves in Trinitrotoluene," Shock Waves **9** (4), 227–237 (1999).
35. R. L. Gustavsen, S. A. Sheffield, and R. R. Alcon, "Detonation Wave Profiles in HMX Based Explosives," AIP Conf. Proc. **429**, 739–744 (1998); http://doi.org/10.1063/1.55674.
36. A. P. Ershov, A. O. Kashkarov, E. R. Pruuel, N. P. Satonkina, V. V. Sil'vestrov, A. S. Yunoshev, and A. V. Plastinin, "Nonideal Detonation Regimes in Low Density Explosives," J. Appl. Phys. **119** (7), 075903(1–6) (2016).
37. K. Tanaka, "Detonation Properties of Condensed Explosives Computed Using the Kihara–Hikita–Tanaka Equation of State," in *Tech. Rep. National Chemical Laboratory for Industry, Tsukuba Research Center* (Tsukuba, Japan, 1983), p. 304.
38. S. G. Andreev, A. V. Babkin, F. A. Baum, N. A. Imkhovik, I. F. Kobylkin, V. I. Kolpakov, S. V. Ladov, V. A. Odintsov, L. P. Orlenko, V. N. Okhitin, V. V. Selivanov, V. S. Solov'ev, K. P. Stanyukovich, V. P. Chelyshev, and B. I. Shekhter, *Physics of Explosion* (Fizmatlit, Moscow, 2004), Vol. 1 [in Russian].
39. A. V. Utkin, S. A. Kolesnikov, and S. V. Pershin, "Effect of the Initial Density on the Structure of Detonation Waves in Heterogeneous Explosives," Fiz. Goreniya Vzryva **38** (5), 111–118 (2002) [Combust., Expl., Shock Waves **38** (5), 590–597 (2002)].
40. V. M. Titov, E. R. Pruuel, K. A. Ten, L. A. Luk'yanchikov, L. A. Merzhievsky, B. P. Tolochko, V. V. Zhulanov, and L. I. Shekhtman, "Experience of using Synchrotron Radiation for Studying Detonation Processes," Fiz. Goreniya Vzryva **47** (6), 3–15 (2011) [Combust., Expl., Shock Waves **47** (6), 615–626 (2011)].
41. E. R. Pruuel, K. A. Ten, B. P. Tolochko, L. A. Merzhievskii, L. A. Luk'yanchikov, V. M. Aul'chenko, V. V. Zhulanov, L. I. Shekhtman, and V. M. Titov, "Implementation of the Capability of Synchrotron Radiation in a Study of Detonation Processes," Dokl. Akad. Nauk **448** (1), 38–42 (2013) [Dokl. Phys. **58** (1), 24–28 (2013)].
42. D. V. Mil'chenko, V. A. Gubachev, L. A. Andreevskikh, S. A. Vakhmistrov, A. L. Mikhailov, V. A. Burnashov, E. V. Khaldeev, A. I. Pyatoikina, S. S. Zhuravlev, and V. N. German, "Nanostructured Explosives Produced by Vapor Deposition: Structure and Explosive Properties," Fiz. Goreniya Vzryva **51** (1), 96–101 (2015) [Combust., Expl., Shock Waves **51** (1), 80–85 (2015)].
43. N. P. Satonkina, A. P. Ershov, A. V. Plastinin, A. S. Yunoshev, "Chemical Reaction Zone and Electrical Conductivity Profile in Detonating High Explosives," Combust. Flame **206**, 249–251 (2019).
44. S. D. Gilev and A. M. Trubachev, "High Electrical Conductivity of TNT Detonation Products," Zh. Tekh. Fiz. **71** (9), 123–127 (2001).

45. D. L. Ornellas, "Calorimetric Determinations of the Heat and Products of Detonation for Explosives: October 1961 to April 1982," Tech. Report (Lawrence Livermore Laboratory, Livermore, 1982), p. 82.
46. Y. Nomura and R. Kawamura, "Soot Derived from the Detonation of a Trinitrotoluene Charge," Carbon **22** (2), 189–191 (1984).
47. A. O. Kashkarov, E. R. Pruuel, K. A. Ten, I. A. Rubtsov, E. Yu. Gerasimov, and P. I. Zubkov, "Transmission Electron Microscopy and X-ray Diffraction Studies of the Detonation Soot of High Explosives," J. Phys.: Conf. Ser. **774**, 012072 (2016).
48. N. P. Satonkina, A. P. Ershov, A. O. Kashkarov, and I. A. Rubtsov, "Elongated Conductive Structures in Detonation Soot of High Explosives," RSC Adv. **10**, 17620–17626 (2020).
49. A. P. Ershov and A. L. Kupershtokh, "Fractal Structure Formation in Explosion," Fiz. Goreniya Vzryva, **27** (2), 111–117 (1991) [Combust., Expl., Shock Waves **27** (2), 231–236 (1991)].
50. N. P. Satonkina, "The Dynamics of Carbon Nanostructures at Detonation of Condensed High Explosives," J. Appl. Phys. **118**, 245901 (2015).
51. N. P. Satonkina, "Correlation of Electrical Conductivity in the Detonation of Condensed Explosives with their Carbon Content," Fiz. Goreniya Vzryva **52** (4), 129–133 (2016) [Combust., Expl., Shock Waves **52** (4), 488–492 (2016)].
52. N. P. Satonkina and D. A. Medvedev, "On the Mechanism of Carbon Nanostructures Formation at Reaction of Organic Compounds at High Pressure and Temperature," AIP Adv. **7** (8), 085101 (2017).
53. V. F. Anisichkin, "Isotope Studies of the Detonation Mechanisms of TNT, RDX, and HMX," Fiz. Goreniya Vzryva **43** (5), 96–103 (2007) [Combust., Expl., Shock Waves **43** (5), 580–586 (2007)].
54. V. F. Anisichkin, "On the Mechanism of the Detonation of Organic High Explosives," Khim. Fiz. **35** (6), 30–34 (2016) [Russ. J. Phys. Chem. **10**, 451–455 (2016); https://doi.org/10.1134/S1990793116030155].